The Level Set Method for Simulating Thin Flow Down an Incline

by

Gurpreet Gosal

A research paper
presented to the University of Waterloo
in partial fulfillment of the
requirement for the degree of
Master of Mathematics
in
Computational Mathematics

Supervisors: Prof. Justin Wan, Prof. Serge D'Alessio

Waterloo, Ontario, Canada, 2016

I hereby declare that I am the sole author of this report. This is a true copy of the report, including any required final revisions, as accepted by my examiners.

I understand that my report may be made electronically available to the public.

Abstract

Fluid dynamics is a very diverse field with its applications in all aspects of our lives from natural phenomenon to cutting edge technology we use. For solving a particular fluid flow problem, we often use computational models to simulate the fluid flow by discretizing the governing equations over its domain. In this work we are dealing with Newtonian fluids, so we derive the governing equation for our problem from standard Navier-Stokes equations. We are particularly interested in thin film flows, especially when thin layer of fluid is flowing under the influence of gravity on an inclined surface. We propose a fluid solver that simulates steady state flow of an instance of thin film flows such that a thin film of water flowing down an incline. We solve this problem as a two-phase flow problem in order to model the influence of air on the thin film flow. One of the primary issue with two-phase flows is how to capture the interface between two fluids, and to do this we use level set method. Once we have our computational model, we compare the findings with theoretical results to validate our model.

Acknowledgements

I would to express my sincere gratitude to my supervisors Prof. Justin Wan and Prof. Serge D'Alessio who always provided their valuable inputs in this research whenever I found myself stuck in a problem. I also appreciate their support, motivation and encouragement throughout the CM program.

I would also like to thank Prof. Kevin Hare, Prof. Arne Storjohann and Stephanie Martin from Department of Computational Mathematics for their administrative and personal support.

I thank my parents and sisters for their constant support throughout this degree.

Last but not the least, I would like to thank all the CM class of 2016, who have become some of my closest friends, for their valuable inputs and jest towards this research!

Table of Contents

List of Figures

Chapter 1

Introduction

The phenomenon of thin film flow is ubiquitous in nature and technologies and therefore it is vital to comprehend the mechanics behind it. Thin films are known to render a multitude of dynamic behaviour such as periodic waves, shock formation, and chaotic structures etc., which has attracted a lot of attention from the research community from theoretical standpoint as well technological applications. Recently there have been a lot of interest in microfluidics and nanofluidics [6],[7] which require computations pertaining to thin film flows. Reynolds was first to investigate the thin film flows in the form of lubrication flows in the 19th century [20].

Typically a thin film flow constitutes a very thin layer of denser liquid partially bounded by a solid substrate and a free surface where the liquid is in contact with another fluid usually a gas or a rarer fluid. In most cases, the thickness, H in the vertical direction is much smaller than the characteristic length, L, in the other direction. For example a thin flow flowing on a very large surface of length L under the influence of gravity and the thickness of fluid layer is H ($H \ll L$). Typically, the magnitude of the velocity field in directions perpendicular to the solid surface is much smaller than the flow velocity along the surface. The most common approach in literature to model such flows is through the momentum equations known as the Navier-Stokes equations when fluids involved are Newtonian.

The major applications of thin film flow have been in engineering applications for instance distillation units and condensers [9], other applications include gravity currents [12], snow avalanches [1], lava flows [2], and in biological settings such as lung airways [8] etc.

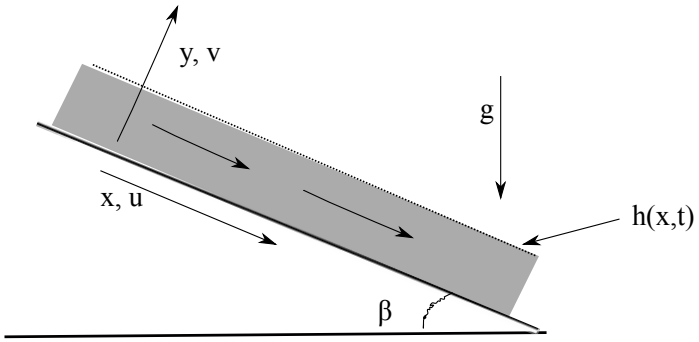

Figure 1.1: Configuration of a thin film flow down an incline in steady state

1.1 Problem Description

In our thin film flow problem we consider laminar flow of a thin fluid film driven by gravitation flowing down an incline. The primary goal is to investigate velocity field and pressure in steady state and to compare them to theoretical results. This will validate the two phase flow solver implemented using level set method for a thin film flow down an incline. Since the flow is shallow, the Navier-Stokes equations are approximated/ simplified. For accurately representing a steady thin film flow, the applied mathematical model must include the relevant physical factors and should also have high degree of complexity essential to capture the spatiotemporal coupling. But the governing equations can be further simplified through valid physical justifications of the phenomenon leading to more precise mathematical model. A very widely used approach is that the space dimensionality of the problem is reduced by assuming shallowness of the flow and forcing a depth integration of the governing equations.

The flow profile under investigation is not given any perturbation initially, as velocity field and pressure are set at zero level. Instead the fluid is allowed to flow in the presence of gravity due to inclination. The nature of the u,v, and p at the steady state is to be investigated and that is the goal of this research. In the Figure 1.1 we have represented this scenario where β is the angle of inclination, g is the gravity acting upon the flow, u,v and p are horizontal velocity field, vertical velocity field and pressure, respectively. $h(x,t)$ represents the interface which varies with time but since we are interested in steady state flow, there shouldn't be any movement in interface and this will be verified in the results section.

1.2 Fluid Interface

Dynamic and free boundaries have garnered tremendous focus from the research community in multi-phase fluid simulation. Scientists are not only interested in mass and momentum transportation of the flow, but they consider it to be vital for fluid flow problem to locate the sharp interfaces between the components of fluids and track their evolution in time. By definition, an interface is an implicit surface that separates two or more fluids in the case of multi-fluid mixture. In order to effectively track the dynamic behaviour of these interfaces, specially crafted algorithms are required.

The technique called *Interface tracking* is developed to tackle this challenge, which is in fact a visualization technique that allows for the identification and tracing of the dynamics of fluid. This technique has been proven successful in the fields as varied as biology, nanotechnology, chemical engineering, computer graphics, combustion etc. In the literature, three principal methodologies are adopted for multi-fluid mixture interface tracking known as *front tracking method*, *volume of fluid method*, and *level set method*.

Front Tracking Method [28, 25, 4] advects the marked interface from an initial configuration and keeps the topology of the interface during the simulation. Therefore, this method is limited to topological changes in multiphase-fluid, such as merging or breaking of droplets. Thus we will not include it in our discussion.

Volume of Fluid Methods [10] is one of best established interface volume tracking method currently in use [11, 19]. As name indicated, it keeps track of the volume of each fluid phase with a sub-volume. This method is therefore based on subcells or sub-volumes, and one tracks the volume percentage that one type of fluid takes up a sub volume cell.

Level Set Method was first proposed by Osher and Sethian [17]. The interface is defined as the zero set of isosurface of the given scalar field [18]. Sethian [22] incorporated the level set method into fluid simulation. It is vital to maintain the geometrical description of the surface as smooth as possible and to do this a strategy was proposed by Enright et. al. [5] where they integrated Lagrangian marker particles with level set method. The main drawback of the level set method is that the material volume is not well preserved over time as explained in [14].

In our problem we employed level set method for interface tracking which will be discussed in Chapter 2.

Chapter 2

Governing Equations

2.1 Equations for Flow Down an Incline

Again consider the two dimensional (2-D) laminar flow of a viscous incompressible fluid down an incline as shown in Figure 1.1. The governing Navier-Stokes and Continuity equations are [19]:

Continuity Equation

$$\frac{\partial u}{\partial x} + \frac{\partial v}{\partial y} = 0, \tag{2.1}$$

u-momentum equation:

$$\frac{\partial u}{\partial t} + u\frac{\partial u}{\partial x} + u\frac{\partial u}{\partial y} = -\frac{1}{\rho}\frac{\partial p}{\partial x} + g\sin\beta + \nu\left(\frac{\partial^2 u}{\partial x^2} + \frac{\partial^2 u}{\partial y^2}\right), \tag{2.2}$$

v-momentum equation:

$$\frac{\partial v}{\partial t} + u\frac{\partial v}{\partial x} + v\frac{\partial v}{\partial y} = -\frac{1}{\rho}\frac{\partial p}{\partial y} - g\cos\beta + \nu\left(\frac{\partial^2 v}{\partial x^2} + \frac{\partial^2 v}{\partial y^2}\right). \tag{2.3}$$

In the flow governing equations above u and v represent horizontal and vertical velocity fields, p represent pressure, g is gravity, β is the angle of inclination of the incline and ν is the kinematic viscosity. For steady fully developed flow which is uniform in x direction, $u = u(y)$ (since there is no variation of u with x), and $v = 0$ (since there is no vertical

velocity in fluid at the steady state). Then (2.1) is automatically satisfied while (2.2) and (2.3) reduce to:

$$0 = g\sin\beta + \nu\frac{\partial^2 u}{\partial y^2}, \tag{2.4}$$

$$0 = -\frac{1}{\rho}\frac{\partial p}{\partial y} - g\cos\beta. \tag{2.5}$$

Let H be the thickness of fluid layer as shown in Figure 1.1 The solution satisfying no-slip and zero stress at the fluid-air interface [$u = 0$ at $z = 0$, $\dfrac{\partial u}{\partial y} = 0$ at $y = H$ and $p = 0$at $y = H$] is:

$$u(y) = \frac{g}{2\nu}\sin\beta(2Hy - y^2), \tag{2.6}$$

$$p(y) = -\rho g cos\beta(y - H). \tag{2.7}$$

Thus, the velocity profile is parabolic and the pressure is hydrostatic. The volume flow rate per unit width (Q) is:

$$Q = \int_0^H u(y)dy = \frac{gH^3 sin\beta}{3\nu}. \tag{2.8}$$

2.1.1 Dimensionless Governing Equations

Previously we looked at a steady fully developed flow, but now let's analyze time variant flow. Here $u = u(x, y, t)$, $v = v(x, y, t)$ and $p = p(x, y, t)$. To cast equations (2.1), (2.2) and (2.3) in dimensionless form we scale the flow variables as follows:

$$(u, v) = (Uu^*, \delta U v^*), \qquad p = \rho U^2 p^*. \tag{2.9}$$

The space and time variables in dimensionless form are as follows:

$$(x, y, t) = (Lx^*, Hy^*, \frac{L}{U}t^*), \qquad p = \rho U^2 p^*, \tag{2.10}$$

where L is a horizontal length scale, $U = \dfrac{Q}{H}$ and $\delta = \dfrac{H}{L} \ll 1$ (i.e. thin fluid layer).

Then (2.1) - (2.3) become (after suppressing (*))

$$\frac{\partial u}{\partial x} + \frac{\partial v}{\partial y} = 0, \tag{2.11}$$

$$\delta Re\left(\frac{\partial u}{\partial t}+u\frac{\partial u}{\partial x}+v\frac{\partial u}{\partial y}\right)=-\delta Re\frac{\partial p}{\partial x}+3+\delta^2\frac{\partial^2 u}{\partial x^2}+\frac{\partial^2 u}{\partial y^2}, \tag{2.12}$$

$$\delta^2 Re\left(\frac{\partial v}{\partial t}+u\frac{\partial v}{\partial x}+v\frac{\partial v}{\partial y}\right)=-Re\frac{\partial p}{\partial y}-3cot\beta+\delta^3\frac{\partial^2 v}{\partial x^2}+\delta\frac{\partial^2 v}{\partial y^2}. \tag{2.13}$$

Equations (2.12) and (2.13) can be rewritten specifically for each medium i.e. water and air. Also the diffusive terms can be written in a way that dynamic viscosity μ is not cancelled to account for the fact that these terms may need to be computed across the interface (we will see this during discretization of momentum equations in Chapter 3):

u-momentum equation:

$$\delta(\frac{\partial u}{\partial t})+\delta(\frac{\partial u^2}{\partial x})+\delta(\frac{\partial uv}{\partial y})=-\delta(\frac{\partial p}{\partial x})+\frac{3}{Re}+\frac{\delta^2}{\mu Re}\frac{\partial}{\partial x}(\mu\frac{\partial u}{\partial x})+\frac{1}{\mu Re}\frac{\partial}{\partial y}(\mu\frac{\partial u}{\partial y}), \tag{2.14}$$

v-momentum equation:

$$\delta^2(\frac{\partial v}{\partial t})+\delta^2(\frac{\partial v^2}{\partial y})+\delta^2(\frac{\partial uv}{\partial x})=-(\frac{\partial p}{\partial y})+\frac{3cot\beta}{Re}+\frac{\delta^3}{\mu Re}\frac{\partial}{\partial x}(\mu\frac{\partial v}{\partial x})+\frac{\delta}{\mu Re}\frac{\partial}{\partial y}(\mu\frac{\partial v}{\partial y}). \tag{2.15}$$

Above equations are applicable for both air and water. Here we have made the assumption that $\delta=\frac{H}{L}\ll 1$ for both air and water but it is largely true only for water whereas in the air it may not hold since H can be large. We can use different δ in air and water and then above equations will have to be modified accordingly when applied for air medium. This is a limitation of our approach which can be addressed in future as an extension of this research.

2.2 Interface Conditions

Having specified the governing equations for the problem, it is vital to look in detail the interface conditions. Consider two fluids as shown in Figure 2.1. It is basically showing the interface between water (L) and air (A). Interface is represented by $y=h(x,t)$ i.e. the height of the interface at location x and time t. Each of the fluid's properties are also

listed in Figure 2.1. Now, along the interface $y = h(x,t)$ we have [16]:

$$p_L + \delta^2 We \frac{h_{xx}}{(1+\delta^2 h_x^2)^{\frac{3}{2}}} - \frac{2}{Re_L(1+\delta^2 h_x^2)}\left[\delta^3 h_x^2 \frac{\partial u_L}{\partial x} + \delta \frac{\partial v_L}{\partial y} - \delta h_x \left(\frac{\partial u_L}{\partial y} + \delta^2 \frac{\partial v_L}{\partial x}\right)\right] = \frac{\rho_A}{\rho_L} p_A - \frac{2\frac{\rho_A}{\rho_L}}{Re_A(1+\delta^2 h_x^2)}\left[\delta^3 h_x^2 \frac{\partial u_A}{\partial x} + \delta \frac{\partial v_A}{\partial y} - \delta h_x \left(\frac{\partial u_A}{\partial y} + \delta^2 \frac{\partial v_A}{\partial x}\right)\right] \tag{2.16}$$

where $We = \dfrac{\sigma H}{\rho_L U^2 H^2}$ is the Weber number, $Re_A = \dfrac{\rho_A U H}{\mu_A}$ is the Reynold's number for air (A) and $Re_L = \dfrac{\rho_L U H}{\mu_L}$ is the Reynold's number for water (L). For water-air interface $\dfrac{Re_L}{Re_A} = 15$, $\dfrac{\rho_A}{\rho_L} = 0.001$. Again note that we are using same δ for air and water for this interface condition; this is a limitation of this work and can be addressed in future.

The above condition is well approximated by:

$$p_L + \delta^2 We \frac{h_{xx}}{(1+\delta^2 h_x^2)^{\frac{3}{2}}} = \frac{\rho_A}{\rho_L} p_A, \tag{2.17}$$

equivalently,

$$\rho_L(p_L + \Delta p) = \rho_A p_A, \tag{2.18}$$

where Δp represents the jump in pressure across the interface due to surface tension. Since, we want to simulate the flow at steady state and in steady state the interface is flat. This implies that $h_{xx} = 0$, so $\Delta p = 0$. This interface condition (2.18) then becomes:

$$\rho_L p_L = \rho_A p_A. \tag{2.19}$$

Also we have interface condition for the velocity [19]:

$$(1-\delta^2 h_x^2)\left(\frac{\partial u_L}{\partial y} + \delta^2 \frac{\partial v_L}{\partial x}\right) - 4\delta^2 h_x \frac{\partial u_L}{\partial x} = \frac{\mu_A}{\mu_L}\left[(1-\delta^2 h_x^2)\left(\frac{\partial u_A}{\partial y} + \delta^2 \frac{\partial v_A}{\partial x}\right) - 4\delta^2 h_x \frac{\partial u_A}{\partial x}\right]. \tag{2.20}$$

For water-air interface $\dfrac{\mu_A}{\mu_L} \approx 0.018$. The above equation (2.20) for interface condition is well approximated by:

$$\frac{\partial u_L}{\partial y} + \delta^2 \frac{\partial v_L}{\partial x} - 4\delta^2 h_x \frac{\partial u_L}{\partial x} = \frac{\mu_A}{\mu_L}\frac{\partial u_A}{\partial y} \tag{2.21}$$

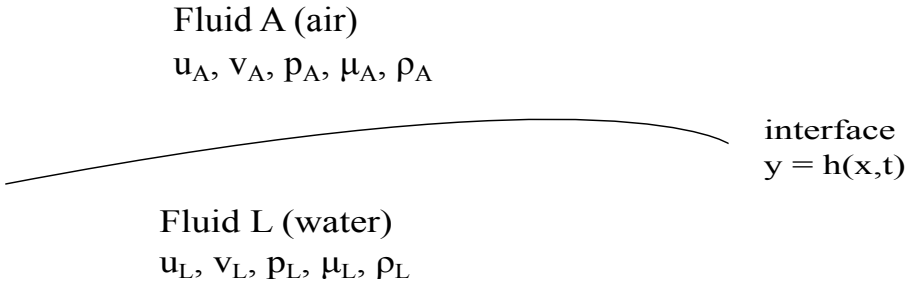

Figure 2.1: Interface between two fluids water and air, $h = h(x, t)$

which can be further simplified to:

$$\mu_L \frac{\partial u_L}{\partial y} = \mu_A \frac{\partial u_A}{\partial y}. \tag{2.22}$$

These interface conditions will be used during discretization of the momentum and continuity equations in Chapter 3. Next we look how interface is tracked between two fluids using level set function.

2.3 Representation and Capturing of Interface Using Level Sets

Continuing from level set method's discussion in Section 1.2, this section presents mathematical formulation of level sets. Consider the representation of the interface between the two fluids (i.e. air and water) using level set function, and how this interface is captured in time when external velocity field acts upon it. This approach approximates solution of time-dependent initial value problem to follow the evolution of the associated level set function whose zero level set always gives the location of the propagating interface.

Suppose we have a function $\phi : \Omega \to R$, with $\Omega \subseteq R^n$, defined such that the zero level set ϕ corresponds to the evolving front $\Gamma(t)$ which is the interface between two fluids. In this way the front is implicitly defined by ϕ. To capture the front evolving with time, we just have to compute ϕ, using an equation which we will discuss shortly, and determine its zero level set and this will be the current topology of the front. More formally, the front Γ is defined as:

$$\Gamma(t) = \{\vec{x} \in \Omega | \phi(\vec{x}, t) = 0\} \tag{2.23}$$

As shown in [24] and [23], the level set fucntion ϕ evolves with time according to the following equation:

$$\phi_t + \vec{u}.\nabla\phi = 0, \tag{2.24}$$

where $\vec{u} = (u, v)$ is the total velocity field. It is shown in [17] that (2.24) accurately displaces the zero level set according to the $\vec{u}$ even in the situations where we might have merging or disintegration of fluid mass.

For the thin film flow problem at hand, we have $\Omega = R^2$, and therefore $\vec{x} = (x, y)$. We consider,

$$\phi(x, y, t) = y - h(x, t), \tag{2.25}$$

where h is a function of x and t. To find the zero level set, set $\phi(x, y, t) = 0$ and we get $y = h(x, t)$ which represents the interface between air and water as shown in Figure 2.1. In this problem we use $h(x, t) = 1$, and we take $\phi < 0$ to be in the water region and $\phi > 0$ in the air: Therefore, we can summarize:

$$\phi(x,t) \begin{cases} > 0 & \forall x \in \text{air} \\ = 0 & \forall x \in \Gamma \\ < 0 & \forall x \in \text{water}. \end{cases} \tag{2.26}$$

Now, in (2.24) we can use the following:

$$\vec{u} = \begin{cases} \vec{u}_L & \forall \phi < 0 \\ \vec{u}_A & \forall \phi > 0. \end{cases} \tag{2.27}$$

We can write (2.24) in simplified form as:

$$\phi_t + u\phi_x + v\phi_y = 0, \tag{2.28}$$

where, ϕ_x and ϕ_y are the derivatives of ϕ w.r.t. x and y, respectively. This is essentially an advection equation which can be solved using upwinding scheme. It will be explained in Chapter 3 when we discuss discretization of level set equation.

Chapter 3

Discretization and Algorithm

Now that we have derived the governing equations for the fluid flow, in this chapter we will describe a finite difference discretization scheme for solving the Navier-Stokes equations shown below:

u-momentum equation:

$$\delta(\frac{\partial u}{\partial t}) + \delta(\frac{\partial u^2}{\partial x}) + \delta(\frac{\partial uv}{\partial y}) = -\delta(\frac{\partial p}{\partial x}) + \frac{3}{Re} + \frac{\delta^2}{\mu Re}\frac{\partial}{\partial x}(\mu\frac{\partial u}{\partial x}) + \frac{1}{\mu Re}\frac{\partial}{\partial y}(\mu\frac{\partial u}{\partial y}), \tag{3.1}$$

v-momentum equation:

$$\delta^2(\frac{\partial v}{\partial t}) + \delta^2(\frac{\partial v^2}{\partial y}) + \delta^2(\frac{\partial uv}{\partial x}) = -(\frac{\partial p}{\partial y}) + \frac{3cot\beta}{Re} + \frac{\delta^3}{\mu Re}\frac{\partial}{\partial x}(\mu\frac{\partial v}{\partial x}) + \frac{\delta}{\mu Re}\frac{\partial}{\partial y}(\mu\frac{\partial v}{\partial y}), \tag{3.2}$$

continuity equation:

$$\frac{\partial u}{\partial x} + \frac{\partial v}{\partial y} = 0. \tag{3.3}$$

Note that these equations are applicable in both fluids (air and water) such that for water Re $= Re_L$, $\mu = \mu_L$ and for air Re $= Re_A$, $\mu = \mu_A$. We will deal with interface terms later in this chapter.

Since for numerical solution of PDEs using finite difference method, we need to move from continuous space to discretized space and define the equations on a finite number of points. There are different finite different approximation schemes that can used to express the partial differential terms in the equations with variable accuracy. Throughout this chapter we will follow the discretization scheme suggested in [13].

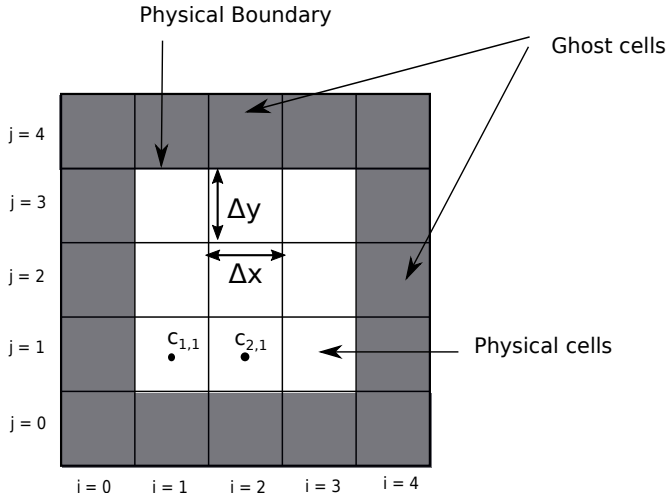

Figure 3.1: Computational domain discretized into a rectilinear grid with $n_x = 3$ and $n_y = 3$. White cells are the physical cells indexed as i = 1,2,...n_x and j = 1,2,...n_y and $c_{1,1}$ and $c_{2,1}$ representing two physical cells. Shaded cells that form strip around the physical domain are ghost cells indexed as i = 0, i = n_x+1 and j = 0, j = n_y+1

3.1 Discretization of the Governing Equations

In our problem we have rectangular computational domain Ω. The computational domain is discretized into a rectilinear grid with rectangular cells $c_{i,j}$ such that i = 1,2,....n_x and j = 1,2,.....n_y. Here Δx is the grid spacing in the x direction and Δy is the grid spacing in y direction. This is shown in Figure 3.1.

It is well known [13, 29] that to ensure stability, u, v and p must be defined at different locations within a cell and this is called a staggered grid. This idea of staggered grid comes from the finite volume method, in which the continuity equation is discretized in each volume cell by considering the mass flux across the cell edges determined by the velocities on these edges. Therefore, in a staggered grid for a cell $c_{i,j}$, $u_{i,j}$, $v_{i,j}$ and $p_{i,j}$ are defined at different locations with $u_{i,j}$ defined at the centre of the right edge, $v_{i,j}$ defined at the centre of top edge and $p_{i,j}$ at the centre of the cell. So, Cell $c_{i,j}$ occupies the spatial region [(i-1)Δx,iΔx] × [(j-1)Δy,iΔy], and the corresponding index (i,j) is assigned to pressure at that cell center as well as to the u-velocity at the right edge and v-velocity at the top edge. Therefore, the pressure value $p_{i,j}$ is located at the coordinates ((i - 0.5)Δx, (j - 0.5)Δy), the horizontal velocity at coordinates (iΔx, (j - 0.5)Δy), and the vertical velocity at the coordinates ((i - 0.5)Δx, jΔy). This staggered grid with discretized variables defined at

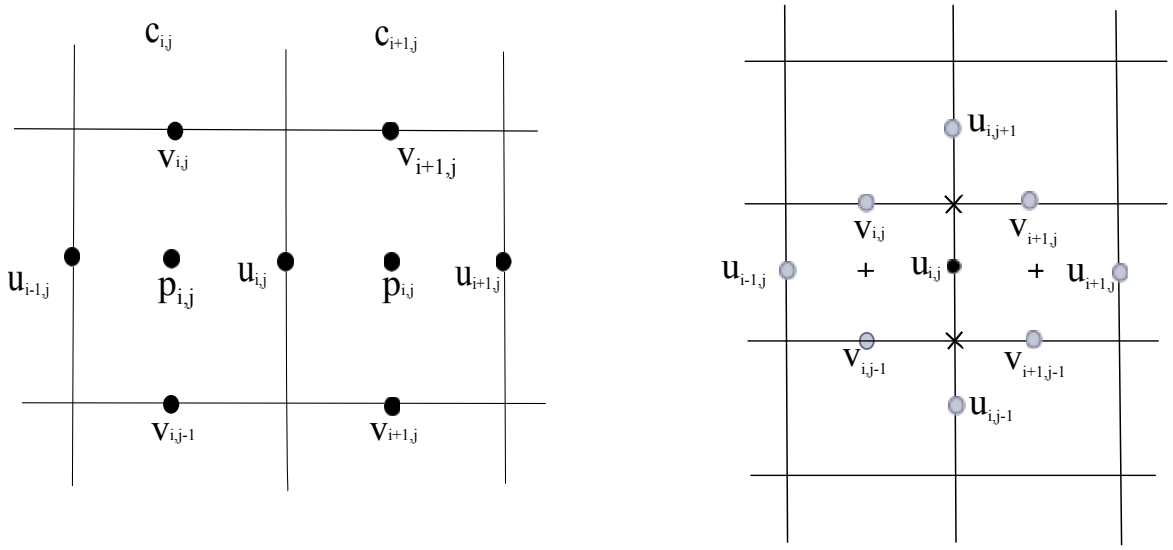

Figure 3.2: Staggered grid is shown on the left with two cells $c_{i,j}$ and $c_{i+1,j}$ p defined at the center, u in the center of left edge and v in the center of top edge for each cell. On the right parameters required for discretization of u-momentum equations are shown

different locations is shown in Figure 3.2.

Although we may not have discretized values of u, v, and p defined on the actual physical boundary, we still need to implement boundary conditions at all the four boundaries. To do this we use the concept of ghost cells. Ghost cells are additional cells added beyond the physical boundary of the domain which do not have any physical significance but they facilitate the implementation of boundary conditions. In Figure 3.1 the dark ribbon of cells around the physical domain represents these ghost cells. Ghost cells are indexed in the same way as the physical cells, and are represented by the indices i = 0, i = n_x+ 1 and j = 0, j = n_y+ 1, as shown in Figure 3.1.

To implement boundary conditions for the quantities not defined at the walls (physical boundaries), ghost cells are utilized. The approach to carry this out will be discussed in Section 3.1.1.

Now, we look at finite difference approximations for the differential terms in the u-momentum (3.1) and v-momentum (3.2) equations. First consider the convective terms i.e. $\delta(\frac{\partial u^2}{\partial x})$, $\delta(\frac{\partial uv}{\partial y})$, $\delta^2(\frac{\partial v^2}{\partial y})$ and $\delta^2(\frac{\partial uv}{\partial x})$. First we deal with the convective terms appearing

in u-momentum equation 3.1. To discretize $\delta(\frac{\partial uv}{\partial y})$ at the midpoint of the right edge of cell $c_{i,j}$ (refer to black dot in Figure 3.2), values for the product uv are required in the two vertical directions. A good solution is to consider the averages of u and v taken at the locations marked $\times$ in Figure 3.2, which gives us the discrete term:

$$\left[\delta\left(\frac{\partial uv}{\partial y}\right)\right]_{i,j} := \frac{\delta}{\Delta y}\left(\frac{(v_{i,j}+v_{i+1,j})}{2}\frac{(u_{i,j}+u_{i+1,j})}{2} - \frac{(v_{i,j-1}+v_{i+1,j-1})}{2}\frac{(u_{i,j-1}+u_{i,j})}{2}\right). \tag{3.4}$$

In a similar fashion, we discretize $\delta(\frac{\partial u^2}{\partial x})$ using central difference with half the mesh width of values averaged at the points marked with + in Figure 3.2:

$$\left[\delta\left(\frac{\partial u^2}{\partial x}\right)\right]_{i,j} := \frac{\delta}{\Delta x}\left(\left(\frac{u_{i,j}+u_{i+1,j}}{2}\right)^2 - \left(\frac{u_{i-1,j}+u_{i,j}}{2}\right)^2\right). \tag{3.5}$$

It is observed that convective terms become dominant at high Reynolds number or high velocities, and in order to remedy this a mixture of central differences as specified above and the donor-cell discretization are used thus obtaining following expressions[3]. Remaining two terms $\delta^2(d\frac{\partial v^2}{\partial y})$ and $\delta^2(\frac{\partial uv}{\partial x})$ are also discretized the same way.

For cell $c_{i,j}$ at the center of right edge for $i = 1, 2, ...n_x-1$ and $j = 1, 2, ...n_y$ we set

$$\begin{aligned}\left[\delta\left(\frac{\partial u^2}{\partial x}\right)\right]_{i,j} &:= \frac{\delta}{\Delta x}\left(\left(\frac{u_{i,j}+u_{i+1,j}}{2}\right)^2 - \left(\frac{u_{i-1,j}+u_{i,j}}{2}\right)^2\right)\\ +\gamma\frac{\delta}{\Delta x}&\left(\frac{|u_{i,j}+u_{i+1,j}|}{2}\frac{(u_{i,j}-u_{i+1,j})}{2} - \frac{|u_{i-1,j}+u_{i,j}|}{2}\frac{(u_{i-1,j}-u_{i,j})}{2}\right),\end{aligned} \tag{3.6}$$

$$\begin{aligned}\left[\delta\left(\frac{\partial uv}{\partial y}\right)\right]_{i,j} &:= \frac{\delta}{\Delta y}\left(\frac{(v_{i,j}+v_{i+1,j})}{2}\frac{(u_{i,j}+u_{i,j+1})}{2} - \frac{(v_{i,j-1}+v_{i+1,j-1})}{2}\frac{(u_{i,j-1}+u_{i,j})}{2}\right)\\ &+\gamma\frac{\delta}{\Delta y}\left(\frac{|v_{i,j}+v_{i+1,j}|}{2}\frac{(u_{i,j}-u_{i,j+1})}{2} - \frac{|v_{i,j-1}+v_{i+1,j-1}|}{2}\frac{(u_{i,j-1}-u_{i,j})}{2}\right).\end{aligned} \tag{3.7}$$

Note that index i goes from $i = 1$ to n_x-1 i.e. discretization of convective terms right on the physical boundary is not shown in the above equations.

Similarly for terms $\delta^2(\frac{\partial v^2}{\partial y})$ and $\delta^2(\frac{\partial uv}{\partial x})$, we get for $i = 1, 2, ...n_x$ and $j = 1, 2, ...n_y-1$

$$\begin{aligned}\left[\delta^2\left(\frac{\partial v^2}{\partial y}\right)\right]_{i,j} &:= \frac{\delta^2}{\Delta y}\left(\left(\frac{v_{i,j}+v_{i,j+1}}{2}\right)^2-\left(\frac{v_{i,j-1}+v_{i,j}}{2}\right)^2\right)\\ +\gamma\frac{\delta^2}{\Delta y}&\left(\frac{|v_{i,j}+v_{i,j+1}|}{2}\frac{(v_{i,j}-v_{i,j+1})}{2}-\frac{|v_{i,j-1}+v_{i,j}|}{2}\frac{(v_{i,j-1}-v_{i,j})}{2}\right),\end{aligned} \tag{3.8}$$

$$\begin{aligned}\left[\delta^2\left(\frac{\partial uv}{\partial x}\right)\right]_{i,j} &:= \frac{\delta^2}{\Delta x}\left(\frac{(u_{i,j}+u_{i,j+1})}{2}\frac{(v_{i,j}+v_{i+1,j})}{2}-\frac{(u_{i-1,j}+u_{i-1,j+1})}{2}\frac{(v_{i-1,j}+v_{i,j})}{2}\right)\\ +\gamma\frac{\delta^2}{\Delta x}&\left(\frac{|u_{i,j}+u_{i,j+1}|}{2}\frac{(v_{i,j}-v_{i+1,j})}{2}-\frac{|u_{i-1,j}+u_{i-1,j+1}|}{2}\frac{(v_{i-1,j}-v_{i,j})}{2}\right).\end{aligned} \tag{3.9}$$

The parameter γ in the above equations ranges between 0 and 1. For $\gamma = 0$, we recover the central difference discretization and for $\gamma = 1$, a pure donor-cell scheme is rendered. In [3] authors suggest that γ should be chosen as per the following inequality:

$$\gamma \geq \underset{i,j}{max}\left(\left|\frac{u_{i,j}\Delta t}{\partial x}\right|,\left|\frac{u_{i,j}\Delta t}{\partial y}\right|\right). \tag{3.10}$$

where we chose γ to be 0.9.

3.1.1 Boundary Conditions for the Discrete Equations

In this section boundary conditions for u,v and p are discussed. The problem is periodic in the x-direction and therefore periodic boundary conditions are implemented in this direction. In section 3.2, u and v updates at each time step are presented and we will see that $u_{n_x,j}\ \forall\ j = 0, 1...n_y+1$ is not updated instead we will compute it using periodic boundary condition. Therefore, we get following condition for u

$$u_{n_x,j} = u_{0,j} \qquad \forall j = 0, 1...n_y+1. \tag{3.11}$$

Similarly, v is also periodic in x-direction. For u the grid points go from $u_{0,j}$ to $u_{n_x,j}$ (where j = 1,2,...n_y) in the x-direction and they all lie in the physical domain thus defined

on physical cells (refer to Figure 3.1 and Figure 3.2). But in the case of v we have $v_{0,j}$ and $v_{n_x+1,j}$ as the ghost values defined on the top edges of ghost cells shown in Figure 3.1. Therefore, to ensure periodicity for v, periodic boundary conditions must also update the ghost cell values. This is implemented as follows:

$$v_{0,j} = v_{n_x-1,j} \qquad \forall j = 0, 1...n_y, \tag{3.12}$$

$$v_{1,j} = v_{n_x,j} \qquad \forall j = 0, 1...n_y, \tag{3.13}$$

$$v_{n_x+1,j} = v_{2,j} \qquad \forall j = 0, 1...n_y. \tag{3.14}$$

Next, consider pressure p, same procedure is followed for p as with v due to presence of ghost cells and we implement the boundary conditions as follows:

$$p_{0,j} = p_{n_x-1,j} \qquad \forall j = 0, 1...n_y+1, \tag{3.15}$$

$$p_{1,j} = p_{n_x,j} \qquad \forall j = 0, 1...n_y+1, \tag{3.16}$$

$$p_{n_x+1,j} = p_{2,j} \qquad \forall j = 0, 1...n_y+1. \tag{3.17}$$

At the bottom boundary, we use no-slip condition for u and v whereas for p we use Neumann boundary condition. The pressure Poisson equation is derived from the momentum equation (which will see in Section 3.2.2). Because it is derived by taking the divergence of the momentum equations, it requires that the solution be sufficiently smooth up to the boundary. The pressure equation, for sufficiently smooth solutions, is equivalent to the continuum Navier-Stokes equation in the non-steady case. For the steady case, note that equivalence is achieved when the pressure Poisson equation is written without the viscosity term and a divergence free boundary condition is enforced for the velocity. We already know the boundary conditions for the velocity field, and now we need boundary conditions for both the velocity field of flow and the pressure that allow us to develop the velocity field in time for a given pressure and then solve for the pressure at each fixed time given the velocity. For an incompressible fluid Neumann boundary condition is used for pressure and the pressure is calculated up to an arbitrary additive constant. Also from numerical solution point of view, the actual pressure exerted on the wallboundary is not known and not possible to find. So the boundary pressure value is commonly assigned the inner grid point value, which means the Neumann B.C. is applied.

Since, u is not defined at the actual physical boundary at the bottom as shown in Figure 3.2, we update the u value in the ghost cell such that average of the $u_{i,0}$ and $u_{i,1}$ is 0 as follows:

$$u_{i,0} = -u_{i,1j} \qquad \forall i = 0, 1...n_x. \tag{3.18}$$

For v at the bottom boundary,

$$v_{i,0} = 0 \qquad \forall i = 0, 1...n_x{+}1, \tag{3.19}$$

and for p at the bottom boundary,

$$p_{i,0} = p_{i,1j} \qquad \forall i = 0, 1...n_x{+}1. \tag{3.20}$$

Now, consider the boundary conditions at the top boundary, We use free slip condition for u and v, and Neumann for pressure. Free slip for u at top is implemented as:

$$u_{i,n_y+1} = u_{i,n_y j} \qquad \forall i = 0, 1...n_x. \tag{3.21}$$

For v at the top boundary,

$$v_{i,n_y} = v_{i,n_y-1} \qquad \forall i = 0, 1...n_x{+}1, \tag{3.22}$$

and for p at the top

$$p_{i,n_y+1} = p_{i,n_y} \qquad \forall i = 0, 1...n_x{+}1. \tag{3.23}$$

3.1.2 Discretization of the Time Derivatives and Stability Condition

Again consider equations (3.1) and (3.2). We have not discretized the time derivative terms i.e. $\left[\delta\frac{\partial u}{\partial t}\right]_{i,j}$ and $\left[\delta^2\frac{\partial v}{\partial t}\right]_{i,j}$. In this section we will look at this. We partition the time domain [0, t_{end}] into equal intervals [nΔt,$(n{+}1)\Delta t$], with n = 0,1,...$t_{end}/\Delta t{-}1$. This implies that we only consider values u, v and p at discrete time points given by nΔt. Therefore, we will time step as $t_k = t_{k-1} + \Delta$t until we reach t_{end}. We perform time discretization as follows:

$$\left[\delta\frac{\partial u}{\partial t}\right]^{n+1}_{i,j} := \frac{u^{n+1}_{i,j} - u^n_{i,j}}{\Delta t}, \qquad \left[\delta\frac{\partial v}{\partial t}\right]^{n+1}_{i,j} := \frac{v^{n+1}_{i,j} - v^n_{i,j}}{\Delta t} \tag{3.24}$$

where superscripts designate the time level.

Adaptive time stepping is preferred where at each time level, Δt is computed using the following conditions [26]:

$$\Delta t < \frac{Re}{2}\left(\frac{1}{\Delta x^2} + \frac{1}{\Delta x^2}\right)^{-1}, \quad \Delta t < \frac{\Delta x}{|u_{max}|}, \quad \Delta t < \frac{\Delta y}{|v_{max}|} \tag{3.25}$$

where, the conditions involving $|u_{max}|$ and $|v_{max}|$ are essentially the Courant-Friedrich-Lewy (CFL) conditions. First condition in equation (3.25) involves the Reynold's number Re, and since it is a two-phase flow problem we have two fluids. Therefore, this condition is computed separately for Re_A (Reynold's number of air) and Re_L (Reynold's number of air) leading to the following time-step selection criteria:

$$\Delta t = min\left\{\frac{Re_L}{2}\left(\frac{1}{\Delta x^2}+\frac{1}{\Delta x^2}\right)^{-1}, \frac{Re_A}{2}\left(\frac{1}{\Delta x^2}+\frac{1}{\Delta x^2}\right)^{-1}, \frac{\Delta x}{|u_{max}|}, \frac{\Delta y}{|v_{max}|}\right\}. \tag{3.26}$$

This is a very restrictive condition on time step and to relax this condition, viscous terms can be considered implicitly in future work.

3.1.3 Discretization of Level Set Funciton

In Section 2.3, we saw how a level set function can be used to capture the interface between two fluids. Now lets look at the discretization of the ϕ. The discretized level set function is defined at the cell centers $c_{i,j}$ same as p. When ϕ is initialized, it should split the domain Ω into two regions. In our problem, we used the convention as described in equation (2.26) that $\phi < 0$ corresponds to water and $\phi > 0$ corresponds to air. ϕ is initialized such that its zero level set is a flat surface. Our domain in y-direction is $y \in [0, 2]$, and we initialize the level set function $\phi(x, y, t)$ as described in equation (2.25) such that $h(x, t = 0) = 1$. This can be expressed as follows:

$$\begin{aligned} \phi(x, y, t = 0) &= y - h(x, t = 0), \\ \phi(x, y, t = 0) &= y - 1. \end{aligned} \tag{3.27}$$

Since, ϕ values are stored at cell centers and the fact that we have to advect the level set according to (2.28), the velocity field must be approximated to the cell centers using interpolation. The simplified form of level set time evolution equation (2.28) can then be discretized as follows:

$$\left[\frac{\partial \phi}{\partial t}\right]_{i,j} + \widetilde{u}_{i,j}\left[\frac{\partial \phi}{\partial x}\right]_{i,j} + \widetilde{v}_{i,j}\left[\frac{\partial \phi}{\partial y}\right]_{i,j} = 0. \tag{3.28}$$

Note that we have used $\widetilde{u}$ and $\widetilde{v}$ in the above equations. It is because $\phi_{i,j}$ and $u_{i,j}$, $v_{i,j}$ are not defined at same points in a cell as shown in the staggered grid in Figure 3.2. Here,

$\widetilde{u}_{i,j}$ and $\widetilde{v}_{i,j}$ represent u and v values approximated at cell centers. Thus, $\widetilde{u}_{i,j}$ and $\widetilde{v}_{i,j}$ are computed as:

$$\begin{aligned} \widetilde{u}_{i,j} &= \frac{u_{i-1,j} + u_{i,j}}{2}, \\ \widetilde{v}_{i,j} &= \frac{v_{i,j-1} + v_{i,j}}{2}. \end{aligned} \tag{3.29}$$

The time derivative term $\left[\frac{\partial \phi}{\partial t}\right]_{i,j}$ is discretized using Forward Euler approximation:

$$\left[\frac{\partial \phi}{\partial t}\right]_{i,j} = \frac{\phi_{i,j}^{n+1} - \phi_{i,j}^{n}}{\Delta t}. \tag{3.30}$$

To approximate the spatial derivative terms, we use upwinding finite differencing details of which can be found in [27]. We get,

$$\left[\frac{\partial \phi}{\partial x}\right]_{i,j} \begin{cases} \frac{\phi_{i,j}^{n} - \phi_{i-1,j}^{n}}{\Delta x}, & \text{if} \quad \widetilde{u}_{i,j} > 0, \\ \frac{\phi_{i+1,j}^{n} - \phi_{i,j}^{n}}{\Delta x}, & \text{if} \quad \widetilde{u}_{i,j} \leq 0, \end{cases} \tag{3.31}$$

and

$$\left[\frac{\partial \phi}{\partial y}\right]_{i,j} \begin{cases} \frac{\phi_{i,j}^{n} - \phi_{i,j-1}^{n}}{\Delta y}, & \text{if} \quad \widetilde{v}_{i,j} > 0, \\ \frac{\phi_{i,j+1}^{n} - \phi_{i,j}^{n}}{\Delta y}, & \text{if} \quad \widetilde{v}_{i,j} \leq 0. \end{cases} \tag{3.32}$$

Above method can be very dissipative and the fluid mass can be lost when simulations are performed for longer time but that is only the case when we have finite domain in all the directions and in such case Finite Volume Method is preferred. But since in our case we have infinite flow in x-direction, it is not a concern and it is safe to use the above discretization for level set function.

3.2 Algorithm Description

Now that we have all the tools required to run our fluid simulations, with the exception of second order differential terms appearing in momentum equations (3.1) and (3.2) which we will discuss in Section 3.2.3. Let's have a detailed look at the structure of the algorithm that we propose to solve this thin film flow problem [13].

3.2.1 The Time-Stepping Loop

Unknowns p, u and v are initialized at $t = 0$ and time is incremented by Δt, as discussed in the previous section on time stepping, until $t = t_{end}$. At time level t_n values of all the parameters are known and these values can be used to perform computations for the time level t_{n+1}. The time-stepping procedure is contained in the proposed algorithm and we refer to it by time-stepping loop.

Time stepping loop is initiated by first performing the time discretization (3.24) of the terms $\left[\delta\frac{\partial u}{\partial t}\right]$ and $\left[\delta^2\frac{\partial v}{\partial t}\right]$ in the momentum equations (3.1) and (3.2):

$$\delta u^{n+1} = \delta u^n + \Delta t\left[\frac{\delta^2}{\mu Re}\frac{\partial}{\partial x}(\mu\frac{\partial u}{\partial x}) + \frac{1}{\mu Re}\frac{\partial}{\partial y}(\mu\frac{\partial u}{\partial y}) - \delta(\frac{\partial u^2}{\partial x}) - \delta(\frac{\partial uv}{\partial y}) + \frac{3}{Re} - \delta(\frac{\partial p}{\partial x})\right], \tag{3.33}$$

$$\delta^2 v^{n+1} = \delta^2 u^n + \Delta t\left[\frac{\delta^3}{\mu Re}\frac{\partial}{\partial x}(\mu\frac{\partial v}{\partial x}) + \frac{\delta}{\mu Re}\frac{\partial}{\partial y}(\mu\frac{\partial v}{\partial y}) - \delta^2(\frac{\partial v^2}{\partial y}) - \delta^2(\frac{\partial uv}{\partial x}) + \frac{3cot\beta}{Re} - (\frac{\partial p}{\partial y})\right]. \tag{3.34}$$

Again note that above equations are valid for both the mediums water as well as air. The terms that involve the interface will be considered in next sections. Then we introduce some abbreviations to write the velocity updates in shorthand notation as follows:

$$F^n := \delta u^n + \Delta t\left[\frac{\delta^2}{\mu Re}\frac{\partial}{\partial x}(\mu\frac{\partial u^n}{\partial x}) + \frac{1}{\mu Re}\frac{\partial}{\partial y}(\mu\frac{\partial u^n}{\partial y}) - \delta(\frac{\partial (u^2)^n}{\partial x}) - \delta(\frac{\partial u^n v^n}{\partial y}) + \frac{3}{Re}\right], \tag{3.35}$$

$$G^n := \delta^2 v^n + \Delta t\left[\frac{\delta^3}{\mu Re}\frac{\partial}{\partial x}(\mu\frac{\partial v^n}{\partial x}) + \frac{\delta}{\mu Re}\frac{\partial}{\partial y}(\mu\frac{\partial v^n}{\partial y}) - \delta^2(\frac{\partial (v^2)^n}{\partial y}) - \delta^2(\frac{\partial u^n v^n}{\partial x}) + \frac{3cot\beta}{Re}\right]. \tag{3.36}$$

and we obtain following velocity updates equations :

$$u^{n+1} = \frac{F}{\delta} - \Delta t\frac{\partial p}{\partial x}, \tag{3.37}$$

$$v^{n+1} = \frac{G}{\delta^2} - \frac{\Delta t}{\delta^2}\frac{\partial p}{\partial x}. \tag{3.38}$$

In our time stepping loop we evaluate F and G at the time level t_n, i.e. F^n and G^n, which are computed by using velocities at time level t_n as expressed in equations (3.35) and (3.36). But we use pressure values from the time level t^{n+1}. So, the velocity updates are implicit in terms of pressure which can be written as:

$$u^{n+1} = \frac{F^n}{\delta} - \Delta t \frac{\partial p^{n+1}}{\partial x}, \tag{3.39}$$

$$v^{n+1} = \frac{G^n}{\delta^2} - \frac{\Delta t}{\delta^2} \frac{\partial p^{n+1}}{\partial x} \tag{3.40}$$

To determine pressure p, continuity equation (3.3) is used. Substitute u, v from (3.39) and (3.40) into (3.3), and we obtain the following:

$$\frac{\partial u^{n+1}}{\partial x} + \frac{\partial v^{n+1}}{\partial y} = 0 = \frac{1}{\delta}\frac{\partial F^n}{\partial x} - \Delta t \frac{\partial^2 p^{n+1}}{\partial x^2} + \frac{1}{\delta^2}\frac{\partial G^n}{\partial y} - \frac{\Delta t}{\delta^2}\frac{\partial^2 p^{n+1}}{\partial y^2}. \tag{3.41}$$

After rearranging above equation, it becomes Poisson equation for the pressure p^{n+1} at time t_{n+1}

$$\delta^2 \frac{\partial^2 p^{n+1}}{\partial x^2} + \frac{\partial^2 p^{n+1}}{\partial y^2} = \frac{1}{\Delta t}\left[\delta \frac{\partial F^n}{\partial x} + \frac{\partial G^n}{\partial y}\right], \tag{3.42}$$

where the right hand side H is defined as follows:

$$H^n = \frac{1}{\Delta t}\left[\delta \frac{\partial F^n}{\partial x} + \frac{\partial G^n}{\partial y}\right]. \tag{3.43}$$

Time-stepping loop can be summarized for $(n+1)^{th}$ time step as follows:

Step1: Compute F^n, G^n and then H^n as per (3.35), (3.36) and (3.43), respectively using the the velocities u^n, v^n.
Step2: Solve the Poisson equation (3.43) to compute the pressure at $(n+1)^{th}$ time level i.e. p^{n+1}.
Step3: Evaluate the velocity field at $(n+1)^{th}$ time level i.e. u^{n+1}, v^{n+1} using (3.39), (3.40) and p^{n+1} computed in step 2.

Step 1 of the time-stepping loop still needs to be looked at since the computation of diffusive terms is different near the interface as well as Step 2 where Poisson equation needs to be solved. Next section will focus on the later.

3.2.2 Solution of the Poisson Equation for p^{n+1}

Consider the Poisson equation (3.43). Using central difference scheme it can be approximated as below:

$$\delta^2 \left(\frac{p^{n+1}_{i+1,j} - 2p^{n+1}_{i,j} + p^{n+1}_{i-1,j}}{\Delta x^2} \right) + \left(\frac{p^{n+1}_{i,j+1} - 2p^{n+1}_{i,j} + p^{n+1}_{i,j-1}}{\Delta y^2} \right) = H^n,$$
$$H^n = \frac{1}{\Delta t} \left[\delta \left(\frac{F^n_{i,j} - F^n_{i-1,j}}{\Delta x} \right) + \left(\frac{G^n_{i,j} - G^n_{i,j-1}}{\Delta y} \right) \right]. \tag{3.44}$$

This implies that boundary values for p, F and G are required; i.e. we need the following quantities for full discretization of Poisson equation:

$$\begin{aligned} &p_{0,j}, \quad p_{n_x+1,j} \qquad \forall j = 1, 2, ...n_y, \\ &p_{i,0}, \quad p_{i,n_y+1} \qquad \forall i = 1, 2, ...n_x. \end{aligned}$$

These boundary values for p are computed using boundary conditions in Section 3.1.1 i.e. periodic boundary conditions for side walls and Neumann boundary conditions for top and bottom walls. We also need the following boundary values for F and G:

$$\begin{aligned} &F_{0,j}, \quad F_{n_x,j} \qquad \forall j = 1, 2, ...n_y, \\ &G_{i,0}, \quad G_{i,n_y} \qquad \forall i = 1, 2, ...n_x. \end{aligned}$$

To compute the boundary values for G, since the problem is non-periodic in *y-direction*, $G_{i,0}, G_{i,n_y+1}, \forall i = 1, 2, ...n_x$ are set equal to vertical velocity field values v at the boundary locations [13] and also using (3.36), add δ^2 term. We already know the vertical velocity field at the boundaries at time level t_n:

$$G^n_{i,0} = \delta^2 v^n_{i,0}, \quad G^n_{i,n_y} = \delta^2 v^n_{i,n_y} \qquad \forall i = 1, 2, ...n_x.$$

But for F boundary values we cannot simply use horizontal velocity field values at boundaries. In fact $F_{0,j}$ and $F_{n_x,j}$ are computed just as other F values are computed that don't reside on the boundary. But to do this we need to approximate the differential terms in (3.35). To compute $F^n_{0,j}$ we require $u^n_{-1,j}$, $u^n_{0,j}$ and $u^n_{1,j}$ $\forall j \in \{1, n_y\}$ to be used in the computation convective and diffusive terms in (3.4)-(3.7). Now, we know all these u terms except $u^n_{-1,j}$ which lies outside the left boundary. But since the problem is periodic in *x-direction* we can say that:

$$u^n_{-1,j} = u^n_{n_x-1,j} \qquad \forall j = 1, 2, ...n_y.$$

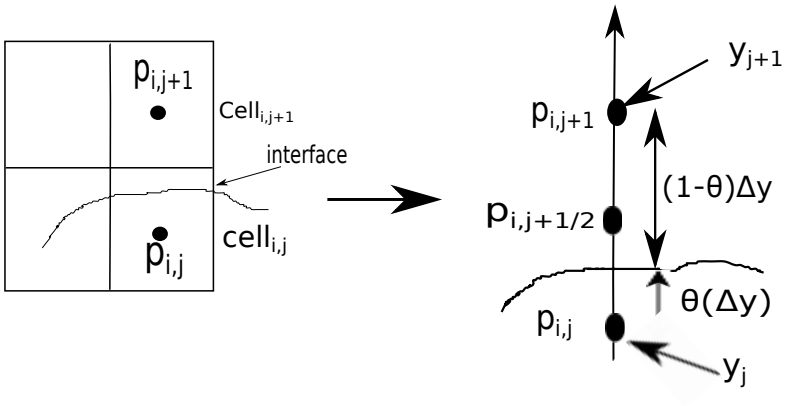

Figure 3.3: Left figure shows interface passing between cells $cell_{i,j}$ and $cell_{i,j+1}$ and a magnified version of the cells on the right shows the pressure values in the two cells. θ is an unknown variable to be determined which reflects how far the interface is from y_j $(\theta\Delta y)$ and from y_{j+1} $(i.e.(\theta+1)\Delta y)$

Similarly, to compute $F^n_{n_x,j}$ we require $u^n_{n_x-1,j}$, $u^n_{n_x,j}$ and $u^n_{n_x+1,j}$ $\forall j \in \{1, n_y\}$. Now, we know all these u terms except $u^n_{n_x+1,j}$ which lies outside the right boundary. Again using the argument of horizontal perioidicity:

$$u^n_{n_x+1,j} = u^n_{1,j} \qquad \forall j = 1, 2, ...n_y.$$

Now, use the above values of $u^n_{-1,j}$ and $u^n_{n_x+1,j}$ and using them in (3.4)-(3.7). This way we compute $F_{0,j}$ and $F_{n_x,j}$.

Next it is vital to consider the situation when computing the derivatives near the interface. Because it is possible that we may have one pressure term in (3.44) lying in denser fluid and the other in rarer fluid. This is shown in Figure 3.3 where $p_{i,j}$ lies in water and $p_{i,j+1}$ lies in air. In that case we can't just use the finite difference approximations as in (3.44). Let's have a detailed perspective of this situation and how it can be resolved.

Near the interface the differential term $\dfrac{\partial^2 p^{n+1}}{\partial y^2}$ in the Poisson equation is approximated as below:

$$\frac{\partial^2 p^{n+1}}{\partial y^2} = \frac{\left(\frac{\partial p}{\partial y}\right)_{i,j+\frac{1}{2}} - \left(\frac{\partial p}{\partial y}\right)_{i,j-\frac{1}{2}}}{\Delta y}. \tag{3.45}$$

Since, $p_{i,j}$ and $p_{i,j-1}$ both lie in the water, it is straightforward to computer the term

$\left(\frac{\partial p}{\partial y}\right)_{i,j-\frac{1}{2}}$ as follows:

$$\left(\frac{\partial p}{\partial y}\right)_{i,j-\frac{1}{2}} = \frac{p_{i,j} - p_{i,j-1}}{\Delta z}. \tag{3.46}$$

But to compute $\left(\frac{\partial p}{\partial y}\right)_{i,j+\frac{1}{2}}$ we need $p_{i,j}$ and $p_{i,j+1}$. Since, $p_{i,j}$ lies in water and $p_{i,j+1}$ in air (as can be seen in Figure 3.3), we will have to utilize the interface condition derived in Section 2.3 which is again stated below:

$$\rho_L p_L + \Delta p = \rho_A p_A,$$

where p_L and ρ_L are pressure and density of water and p_A and ρ_A are pressure and density of air. Ignoring the surface tension due to the fact that we are interested in steady state solution (this was discussed in detail in Chapter 2), we set $\Delta p = 0$. Taking the derivative of the above equaiton we get,

$$\frac{\partial\left(\rho_L p_L\right)}{\partial y} = \frac{\partial\left(\rho_A p_A\right)}{\partial y}, \tag{3.47}$$

or equivalently,

$$\rho_L \frac{\partial\left(p_L\right)}{\partial y} = \rho_A \frac{\partial\left(p_A\right)}{\partial y}. \tag{3.48}$$

Denote the pressure value right at the interface to be p_I as shown in Figure 3.3. We can express the finite difference approximations of the derivatives in the above equations for each medium using p_I as follows:

$$\rho_L \left(\frac{p_I - p_{i,j}}{\theta \Delta y}\right) = \rho_A \left(\frac{p_{i,j+1} - p_I}{(1-\theta)\Delta y}\right), \tag{3.49}$$

such that,

$$\begin{aligned} p_I &= \frac{\rho_A \theta p_{i,j+1} + \rho_L (1-\theta) p_{i,j}}{\widehat{\rho}}, \\ \widehat{\rho} &= \rho_L (1-\theta) + \rho_A \theta. \end{aligned} \tag{3.50}$$

Then,

$$\left(\frac{\partial p}{\partial y}\right)_{i,j+\frac{1}{2}} = \frac{\rho_L}{\rho_A}\left(\frac{p_I - p_{i,j}}{\theta \Delta y}\right) = \frac{\rho_L}{\widehat{\rho}}\left(\frac{p_{i,j+1} - p_{i,j}}{\theta \Delta y}\right). \tag{3.51}$$

Now, we can accurately approximate $\dfrac{\partial^2 p^{n+1}}{\partial y^2}$ by substituting (3.46) and (3.51) in (3.45) and we get the following finite difference approximation

$$\frac{\partial^2 p^{n+1}}{\partial y^2} = \frac{\frac{\rho_L}{\widehat{\rho}}(p^{n+1}_{i,j+1} - p^{n+1}_{i,j}) - (p^{n+1}_{i,j} - p^{n+1}_{i,j-1})}{\Delta y^2}. \tag{3.52}$$

Using similar arguments we find that if the interface lies between $p_{i,j-1}$ (in air) and $p_{i,j}$ (in water) then we get the following:

$$\frac{\partial^2 p^{n+1}}{\partial y^2} = \frac{(p^{n+1}_{i,j+1} - p^{n+1}_{i,j}) - \frac{\rho_L}{\widehat{\rho}}(p^{n+1}_{i,j} - p^{n+1}_{i,j-1})}{\Delta y^2}. \tag{3.53}$$

Reader should note that if the current point i.e. $p_{i,j}$ is in air instead of water then just switch ρ_L in the above two equations with ρ_A.

Similarly, if interface is between $p_{i,j}$ and $p_{i+1,j}$ then we cannot use central difference approximation for $\delta^2 \dfrac{\partial^2 p^{n+1}}{\partial x^2}$ term in poisson equation. Instead same strategy is followed as for $\dfrac{\partial^2 p^{n+1}}{\partial y^2}$. So for the case when interface is between $p_{i,j}$ (in water) and $p_{i+1,j}$ (in air) we get:

$$\delta^2 \frac{\partial^2 p^{n+1}}{\partial x^2} = \delta^2 \left(\frac{\frac{\rho_L}{\widehat{\rho}}(p_{i+1,j} - p_{i,j}) - (p_{i,j} - p_{i-1,j})}{\Delta x^2} \right), \tag{3.54}$$

and if interface is between $p_{i,j}$ (in water) and $p_{i-1,j}$ (in air) we get,

$$\delta^2 \frac{\partial^2 p^{n+1}}{\partial x^2} = \delta^2 \left(\frac{(p_{i+1,j} - p_{i,j}) - \frac{\rho_L}{\widehat{\rho}}(p_{i,j} - p_{i-1,j})}{\Delta x^2} \right). \tag{3.55}$$

If the current point is in air then switch the densities in the above equations.

Now that we have discretized the Poisson equation. The next step is to solve for the pressure. This is a very large sparse system with unknowns containing $n_x n_y$ equations and $n_x n_y$ unknowns. There are various techniques to solve $Ax{=}b$, $A \in R^{n \times n}$ where $n = n_x n_y$. First is *Direct Methods* where runtime depends only on size; independent of data, structure, or sparsity and work well for n up to a few thousand. Then there are *Sparse Direct methods* where runtime depends on size, sparsity pattern; (almost) independent of data and can work well forn up to 10^4 or 10^5 or more. And finally we have *Indirect or Iterative Methods* where runtime depends on data, size, sparsity, required accuracy. They require tuning,

preconditioning and are good choice in many cases. When $n > 10^6$, these are the only choice.

Conjugate Gradient (CG) method is one of the iterative methods, and in this work we used CG. in theory CG.

CG Algorithm

We have a sparse system $Ap=H$
p is the unknown pressure and H is the RHS computed above.

r $\rightarrow$ residual, $\rho_k \rightarrow$ is the 2-norm of residual at k_{th} iteration, $\epsilon \rightarrow$ tolerance, d $\rightarrow$ direction vector
begin
r:= H - Ap, $\rho_0 = \|r\|^2$
for k=1,2,....max-iterations
    quit if $\sqrt{\rho_{k-1}} \leq \epsilon \|b\|$
    if k = 1 then d := r; else d := r + $(\rho_{k-1}/\rho_{k-2})d$
    w := Ad
    $\alpha := \rho_{k-1}/(d^T w)$
    p := p + αd
    r := r - αw
    $\rho_k := \|r\|^2$
return p
end

3.2.3 The Discrete Momentum Equations

We haven't yet discretized the spatial pressure derivatives that occur in the time discretized momentum equations (3.39) and (3.40). We make the following finite difference discretization for those terms:

$$u_{i,j}^{n+1} = \frac{F_{i,j}^n}{\delta} - \frac{\Delta t}{\Delta x}(p_{i+1,j}^{n+1} - p_{i,j}^{n+1}) \quad \forall i = 0, 1, ...n_x - 1 \quad \text{and} \quad j = 1, 2, ...n_y, \tag{3.56}$$

$$v_{i,j}^{n+1} = \frac{G_{i,j}^n}{\delta^2} - \frac{\Delta t}{\delta^2 \Delta y}(p_{i,j+1}^{n+1} - p_{i,j}^{n+1}) \quad \forall i = 1, 2, ...n_x \quad \text{and} \quad j = 1, 2, ...n_y - 1. \tag{3.57}$$

Note that $u_{0,j}$ is explicitly updated but $u_{n_x,j}$ is not since it is computed using the periodic boundary conditions.

In Section 3.1 we saw discretization of the convective terms in equations (3.6)-(3.10). But we have't discretized the diffusive terms $\left[\frac{\delta^2}{\mu Re}\frac{\partial}{\partial x}(\mu\frac{\partial u}{\partial x})\right]$, $\left[\frac{1}{\mu Re}\frac{\partial}{\partial y}(\mu\frac{\partial u}{\partial y})\right]$, $\left[\frac{\delta^3}{\mu Re}\frac{\partial}{\partial x}(\mu\frac{\partial v}{\partial x})\right]$ and $\left[\frac{\delta}{\mu Re}\frac{\partial}{\partial y}(\mu\frac{\partial v}{\partial y})\right]$ which we need for (3.35) and (3.36). We cannot just use central differencing for their discretization because near the interface it is possible that to compute the second derivative we need grid points residing in two different liquids. It is the same scenario we discussed in Poisson equation in Figure 3.3. But instead of variable ρ across the interface we have variable μ. First consider diffusive term $\left[\frac{1}{\mu Re}\frac{\partial}{\partial y}(\mu\frac{\partial u}{\partial y})\right]$ which occur in the update of F (3.35). Let the interface exist between $u_{i,j}$ and $u_{i,j+1}$ and that $u_{i,j}$ is in water and $u_{i,j+1}$ is in air. Since the current grid point is in water, we use Re $= Re_L$ and $\mu = \mu_L$ and we use the following approximation:

$$\left[\frac{1}{\mu_L Re_L}\frac{\partial}{\partial y}(\mu\frac{\partial u}{\partial y})\right]_{i,j} = \frac{1}{\mu_L Re_L}\left[\frac{\left(\mu\frac{\partial u}{\partial y}\right)_{i,j+\frac{1}{2}} - \left(\mu\frac{\partial u}{\partial y}\right)_{i,j-\frac{1}{2}}}{\Delta y}\right], \tag{3.58}$$

where we have,

$$\left(\mu\frac{\partial u}{\partial y}\right)_{i,j-\frac{1}{2}} = \mu_L\left(\frac{u_{i,j} - u_{i,j-1}}{\Delta y}\right). \tag{3.59}$$

Using the stress condition across the interface derived in Chapter 2:

$$\begin{aligned} \mu_L\frac{\partial u}{\partial y} &= \mu_A\frac{\partial u}{\partial y}, \\ \mu_L\left(\frac{u_I - u_{i,j}}{\theta\Delta y}\right) &= \mu_A\left(\frac{u_{i,j+1} - u_I}{(1-\theta)\Delta y}\right) \end{aligned} \tag{3.60}$$

where, u_I is the horizontal velocity field at the interface and θ represents the fraction of Δy that u_I is away from $u_{i,j}$. It is determined as $\theta = \left|\frac{\phi_{i,j}}{\phi_{i,j+1} - \phi_{i,j}}\right|$, where ϕ is the level set function.

Solving for u_I we get,

$$\begin{aligned} u_I &= \frac{\mu_A\theta u_{i,j+1} + \mu_L(1-\theta)ui, j}{\widehat{\mu}}, \\ \widehat{\mu} &= \mu_A\theta + \mu_L(1-\theta). \end{aligned} \tag{3.61}$$

Thus,

$$\begin{aligned}\left(\mu\frac{\partial u}{\partial y}\right)_{i,j+\frac{1}{2}} &= \mu_L\left(\frac{u_I - u_{i,j}}{\theta\Delta y}\right),\\ \left(\mu\frac{\partial u}{\partial y}\right)_{i,j+\frac{1}{2}} &= \frac{\mu_L\mu_A}{\widehat{\mu}\Delta y}(u_{i,j+1} - u_{i,j}).\end{aligned} \tag{3.62}$$

Hence,

$$\left[\frac{1}{\mu_L Re_L}\frac{\partial}{\partial y}(\mu\frac{\partial u}{\partial y})\right]_{i,j} = \frac{\mu_A}{\widehat{\mu}Re_L}\left(\frac{u_{i,j+1} - u_{i,j}}{\Delta y^2}\right) - \frac{1}{Re_L}\left(\frac{u_{i,j} - u_{i,j-1}}{\Delta y^2}\right). \tag{3.63}$$

The above approach can easily be adapted to the scenario where $u_{i,j}$ is in air and $u_{i,j-1}$ is in water, then we have:

$$\begin{aligned}\left[\frac{1}{\mu_A Re_A}\frac{\partial}{\partial y}(\mu\frac{\partial u}{\partial y})\right]_{i,j} &= \frac{\mu_L}{\widehat{\mu}Re_A}\left(\frac{u_{i,j+1} - u_{i,j}}{\Delta y^2}\right) - \frac{1}{Re_A}\left(\frac{u_{i,j} - u_{i,j-1}}{\Delta y^2}\right),\\ \widehat{\mu} &= \mu_L\theta + \mu_A(1-\theta).\end{aligned} \tag{3.64}$$

On the other hand if the interface is between $u_{i,j}$ (in water) and $u_{i,j-1}$ (in air), then we get the following:

$$\left[\frac{1}{\mu_L Re_L}\frac{\partial}{\partial y}(\mu\frac{\partial u}{\partial y})\right]_{i,j} = \frac{1}{Re_L}\left(\frac{u_{i,j+1} - u_{i,j}}{\Delta y^2}\right) - \frac{\mu_A}{\widehat{\mu}Re_L}\left(\frac{u_{i,j} - u_{i,j-1}}{\Delta y^2}\right). \tag{3.65}$$

Similar approach is used for computation of $\left[\frac{\delta^2}{\mu Re}\frac{\partial}{\partial x}(\mu\frac{\partial u}{\partial x})\right]$, $\left[\frac{\delta^3}{\mu Re}\frac{\partial}{\partial x}(\mu\frac{\partial v}{\partial x})\right]$ and $\left[\frac{\delta}{\mu Re}\frac{\partial}{\partial y}(\mu\frac{\partial v}{\partial y})\right]$.

3.2.4 Summary of Two-Phase Flow Solver

Now that we have finite difference discretization of the governing equations for two phase flow down an incline, next we present how each of these components are put together in the form of an algorithm in the fluid solver.

Algorithm for Two-Phase Flow Solver

1. Set t:= 0, n:= 0
2. Assign initial values to u, v, p (in our case they are all initialized at 0 level on the entire grid)
3. **while** $t < t_{end}$
4. Select the timestep Δt according to (3.26)
5. Set boundary values for u, v as per the specifications in Section 3.1.1 for top, bottom and the sides
6. Compute F^n and G^n using updates in (3.35) and (3.36) and while using the appropriate discretization for diffusive terms
7. Compute RHS of the Poisson equation as in (3.44)
8. Solve the pressure equation for p^{n+1} using the CG solver.
9. Compute u^{n+1} and u^{n+1} using (3.56) and (3.57), respectively
10. Advance the level set function for one time step of size Δt using forward upwinding scheme for advection equation.
11. t $\leftarrow$ t + Δt, n $\leftarrow$ n + 1
12. **end while**

Chapter 4

Results

In this chapter, we perform experiments to test the validity of the computational model developed in Chapter 3 by comparing the outcomes with theoretical findings. Parameters in the models are varied and consistency of the experimental results is verified against theoretical results. We assume that the water is flowing down an incline with angle of inclination $\beta = 45°$. Consider incline to be of infinite length, it becomes periodic flow problem. We set the periodicity to be of length 5 in horizontal direction. In vertical direction we assume that thickness of thin film is 1 and therefore the interface is defined at $y = 1$ (3.27). For $1 < y < 2$ we have air. Thus finally we have a box of length of 5 in horizontal direction and of height 2 in vertical direction. The Reynold's number used for water is $Re_L = 1$ and $\frac{Re_A}{Re_L} = \frac{1}{15}$. Also, the dynamic viscosity of water is, $\mu_L = 0.001$ and dynamic viscosities of air μ_A and water μ_L are related by the ratio $\frac{\mu_A}{\mu_L} = 0.018$.

4.1 Theoretical Steady State Solution

As suggested in Chapter 1, we are interested in steady state solution for the thin film of water flowing down an incline shown in Figure 1.1. The idea is to initialize the velocity field and pressure in both air and water to be at zero level and let the thin film of water flow under the influence of gravity. Eventually, a steady state flow will be achieved. In this section we will derive the steady state velocity field and pressure using the governing Navier-Stokes equations. These will be theoretical results which we will later compared with computational results to validate our model.

4.1.1 Steady State Solution for Vertical Velocity Field

First we derive steady state solution using the governing equations (2.11), (2.12) and (2.13). Assuming a steady, unidirectional flow there is no variation of u, v and p with x, so equation (2.11) reduces to:

$$\frac{\partial v}{\partial y} = 0. \tag{4.1}$$

Thus,

$$v = K \tag{4.2}$$

where, K is an arbitrary constant. Due to no-slip boundary condition (3.19) at the bottom, we have $v = 0$ at $y = 0$ for all time levels. But according to (4.1), at steady state $\frac{\partial v}{\partial y} = 0$ which means,

$$v = 0 \quad \forall y \in [0, 2] \wedge \forall x \in [0, 5]. \tag{4.3}$$

This is the vertical velocity field at steady state.

4.1.2 Steady State Solution for Horizontal Velocity Field

Before proceeding to find steady state solution for horizontal velocity field, we introduce some notation to be used throughout this section. Let u_L be the horizontal velocity field in water represented as,

$$u(x, y, t) = u_L(x, y, t) \quad \forall y \in [0, 1] \wedge x \in [0, 5], \tag{4.4}$$

and let u_A be the horizontal velocity field in air such that,

$$u(x, y, t) = u_A(x, y, t) \quad \forall y \in (1, 2] \wedge x \in [0, 5]. \tag{4.5}$$

Now that we have the notation, we proceed to derive theoretical results for horizontal velocity field. As per equation (4.3), $v = 0$ everywhere in the domain in the steady state. Also there is no variation of u, v with x in the steady state due to unidirectional flow assumption. The equation (2.12) reduces to:

$$3 + \frac{\partial^2 u}{\partial y^2} = 0. \tag{4.6}$$

After integrating equation (4.6) twice in water we get :

$$u_L(y) = -\frac{3}{2}y^2 + Cy + D, \tag{4.7}$$

where C, D are constants of integration to be determined. Due to no-slip boundary condition at the bottom boundary, we have $u = 0$ at $y = 0$. Substituting this in (4.7) we get $D = 0$. To determine C, we use zero stress condition at the interface because air is much less dense than water, the stress it imposes is very small and can be neglected in most applications. The zero stress condition is expressed as:

$$\frac{\partial u_L}{\partial y} = 0 \quad \text{at} \quad y = 1. \tag{4.8}$$

After taking derivative of (4.7) w.r.t. y and using (4.8), we get $C = 3$. Therefore, in water we have:

$$u_L(y) = -\frac{3}{2}y^2 + 3y. \tag{4.9}$$

According to (4.9), $u_L(y = 1) = \frac{3}{2}$, and since density of air is very low, shear stress in air is negligible [19]. Therefore, $\mu_A \frac{\partial u_A}{\partial y} = 0$. Due to continuity of velocity at the interface we have $u_L(y = 1) = u_A(y = 1) = \frac{3}{2}$, and since $\frac{\partial u_A}{\partial y} = 0$ in air which implies that:

$$u_A(y) = \frac{3}{2} \quad \forall y \in (1, 2]. \tag{4.10}$$

Steady state horizontal velocity fields derived in (4.9) and (4.10) are applicable under the zero shear stress assumption at the interface and in the air. Next, we consider when we have non-zero shear stress. Again, we integrate (4.6) twice for air and water separately. In the case of water we have,

$$su_L(y) = -\frac{3}{2}y^2 + Cy + D. \tag{4.11}$$

Using no-slip condition at $y = 0$, we get $D = 0$. We are yet to determine C in (4.11) but first consider the horizontal velocity field in air:

$$u_A(y) = -\frac{3}{2}y^2 + Ey + F. \tag{4.12}$$

Applying free-slip condition at $y = 2$,

$$\begin{aligned} \frac{\partial u_A}{\partial y} = 0 \quad \text{at} \quad y = 2, \\ E = 6. \end{aligned} \tag{4.13}$$

So, we have:

$$\begin{aligned} u_L(y) &= -\frac{3}{2}y^2 + Cy, \\ u_A(y) &= -\frac{3}{2}y^2 + 6y + F. \end{aligned} \tag{4.14}$$

There are two constants C and F to be determined yet. We use two conditions at the interface to determine. Condition 1: Stress condition from equation (2.22) which is:

$$\mu_L \frac{\partial u_L}{\partial y} = \mu_A \frac{\partial u_A}{\partial y} \quad \text{at} \quad y = 1.$$

After applying this condition to (4.14), we get:

$$C = 3 + 3(\frac{\mu_A}{\mu_L}). \tag{4.15}$$

Condition 2: Continuity of velocity field across the interface i.e.,

$$u_L(1) = u_A(1).$$

Using the above condition, we find that:

$$F = C - 6 = -3 + 3(\frac{\mu_A}{\mu_L}). \tag{4.16}$$

We finally have,

$$\begin{aligned} u_L(y) &= -\frac{3}{2}y^2 + 3(1 + \frac{\mu_A}{\mu_L})y, \\ u_A(y) &= -\frac{3}{2}y^2 + 6y + 3(-1 + \frac{\mu_A}{\mu_L}). \end{aligned} \tag{4.17}$$

4.1.3 Steady State Solution for Pressure

For steady state pressure solution we consider the momentum equation (2.13). As stated before, u and v are invariant for different x, (2.13) reduces to:

$$\frac{\partial p_L}{\partial y} = -\frac{3cot\beta}{Re_L} \quad \forall y < 1, \tag{4.18}$$

$$\frac{\partial p_A}{\partial y} = -\frac{3cot\beta}{Re_L} \quad \forall y > 1. \tag{4.19}$$

Note that the pressure gradient only depends on Reynold's number of water and angle of inclination of incline. Also, the above pressure gradient value is for the entire domain not only at the boundaries. At the interface, the interface condition derived in Chapter 2 i.e. (2.19) is applicable i.e.,

$$\rho_L p_L = \rho_A p_A.$$

Taking the derivative w.r.t. y we get,

$$\rho_L \frac{\partial p_L}{\partial y} = \rho_A \frac{\partial p_A}{\partial y}. \tag{4.20}$$

We know, $\frac{\partial p_L}{\partial y} = -\frac{3cot\beta}{Re_L}$ and $\frac{\partial p_A}{\partial y} = -\frac{3cot\beta}{Re_A}$ and when the values of the derivatives are substituted in (4.20), we get same left hand side and right hand side which confirms the validity of (4.18) and (4.18).

Also, at steady state pressure should be invariant with x due to our assumption of unidirectional flow and it will be confirmed using the experiments in the next section.

4.2 Simulation Results at Steady State

In this section theoretical steady state solutions derived in the previous section are compared with the simulation results. The goal is to validate the computational model developed in Chapter 3.

4.2.1 Vertical Velocity Field

First we check the vertical velocity field at the steady state which should be zero at all grid points (4.3). Figure 4.1 depicts vertical velocity field at the steady state and agrees with the theoretical result.

4.2.2 Horizontal Velocity Field

For horizontal velocity field u, first we look at time evolution of the velocity field with y. Since, u is invariant with x (which will be experimentally later confirmed in this section), we select a $x = 2.5$ and observe the variation of u with y in time as shown in Figure 4.2. u

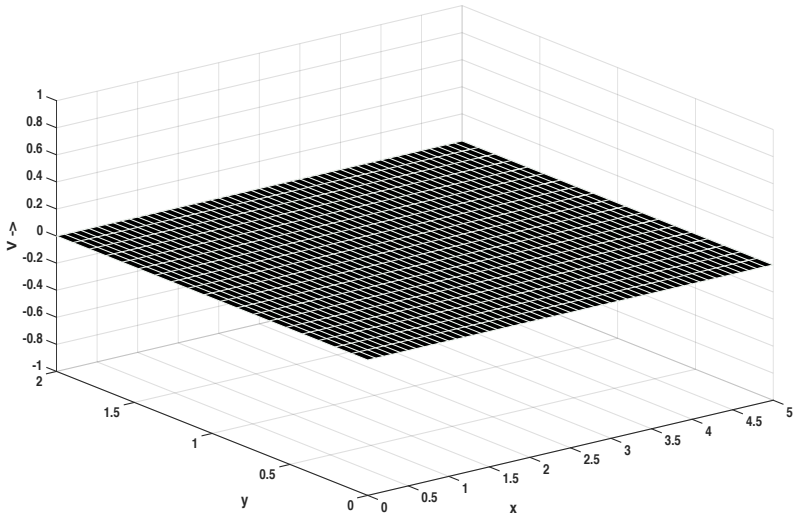

Figure 4.1: Vertical velocity field

is plotted starting from $t = 0$ where $u = 0$ at all values of y, steady state is reached around $t = 4$ as we can see there is very small variation in u between $t = 4$ and $t = 17$. Next we confirm if the nature of the y versus u curve in steady state agrees with the theoretical findings.

To do this, two situations are considered, one when there is zero stress across the interface as well as in the air i.e. (4.10) and (4.9) and another case when there is non-zero stress (4.17). We plot theoretical curves and compare it with the curve obtained from simulations as shown in Figure 4.3.

In Figure 4.3, the solid black curve is the experimental result for u profile whereas dashed red curve is the theoretical result for the zero shear stress condition (4.9) and (4.9). We can see that below the interface at $y = 1$ i.e. in water two curves are overlapping which means there is good agreement between theoretical and experimental results, whereas above the interface i.e. in air, the theoretical u is constant but experimental curve is still parabolic and they are not overlapping although they are very close. The dashed blue curve in Fiigure 4.3 represent theoretical result for variation of u with y but when shear stress is non-zero at the interface (4.17). Again there is good agreement between theoretical result and experimental results inside water but in the air large deviation.

This deviation between theoretical and experimental result needs further investigation

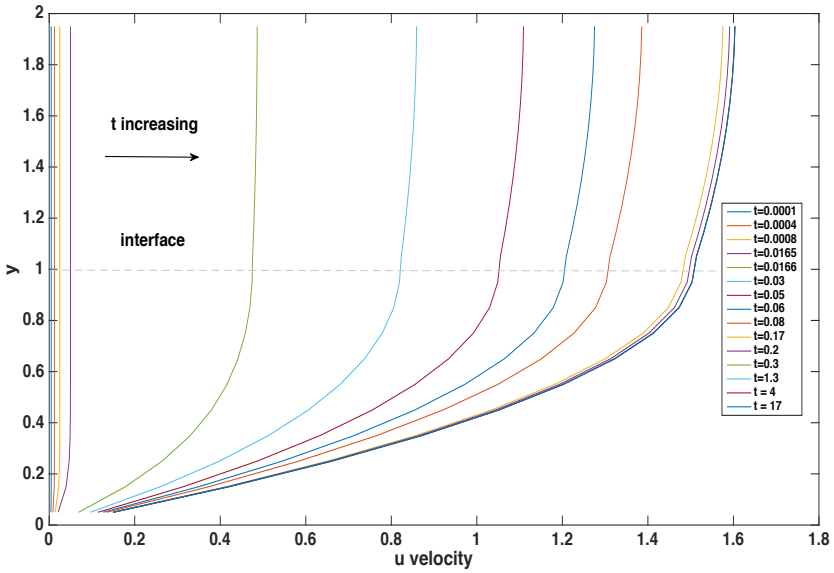

Figure 4.2: Evolution of horizontal velocity u field over time w.r.t. y

but we are not interested in modelling the velocity field in the air as long as significant agreement is achieved for the fields in water which we do for both zero-stress and non-zero stress assumption. From this experiment we can conclude that the zero-stress assumption is more accurate compared to non-zero-stress for the thin flow problem at hand with and the specifications we used.

Another test we do is to check if there is variation of experimental u with x. Because as we can see in equations (4.10), (4.9) as well as (4.17) there is no variation with x. So we plot u at two different x values as shown in Figure 4.4. We can see two curves are overlapping thus confirming the theoretical findings.

The goal of this research was to model u, v and p inside water correctly which is the case.

Finally, we also want to check that if u varies with change in Reynold's number of water and air. We consider two cases here one with $Re_L = 1$ and another with $Re_L = 2$ and $\dfrac{Re_A}{Re_L} = \dfrac{1}{15}$. As it is apparent in (4.10), (4.9) and (4.17) that there is no u dependence on Reynold's number, it should be confirmed for simulation results. Figure 4.5 confirms this finding.

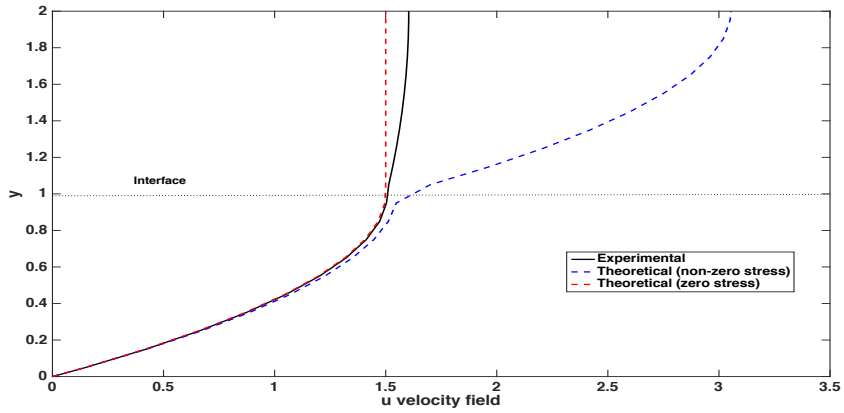

Figure 4.3: Comparison of theoretical steady state velocities with experimental steady state velocity for zero stress and non-zero stress condition

4.2.3 Pressure

Last validation we perform is for the pressure gradient. We validate theoretical pressure gradient found in (4.18) and (4.18). We have:

$$\begin{aligned} \frac{\partial p_L}{\partial y} &= -3, \\ \frac{\partial p_A}{\partial y} &= -3. \end{aligned} \tag{4.21}$$

Firgure 4.6 shows the theoretical versus experimental pressure gradient at all y values. As we can see the theoretical curve (dashed red) $\left[\frac{\partial p}{\partial y}\right]_{theoretical}$ = -3 $\forall y$ whereas experimental result $\left[\frac{\partial p}{\partial y}\right]_{experimental}$ (solid black) is in close agreement with theoretical result except near the interface where there is slight deviation from -3 of the order of 10^{-3}.

So, we have demonstrated that computational model developed in Chapter 2 and 3 is valid and the results achieved largely agree with that of theoretical results.

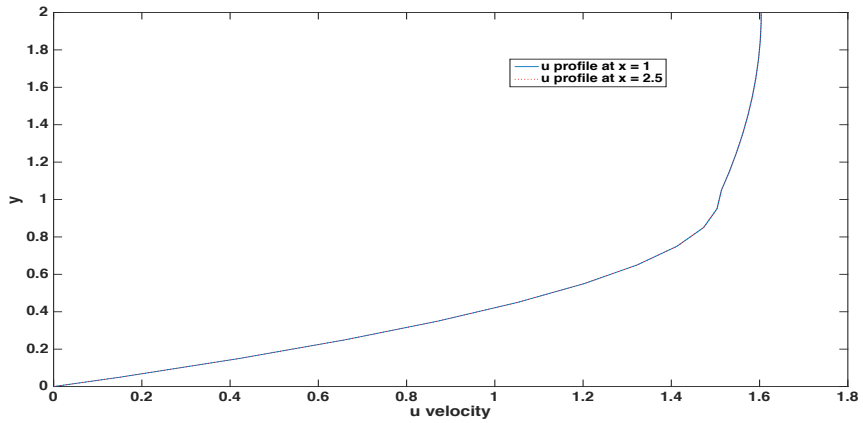

Figure 4.4: horizontal velocity field at different x values

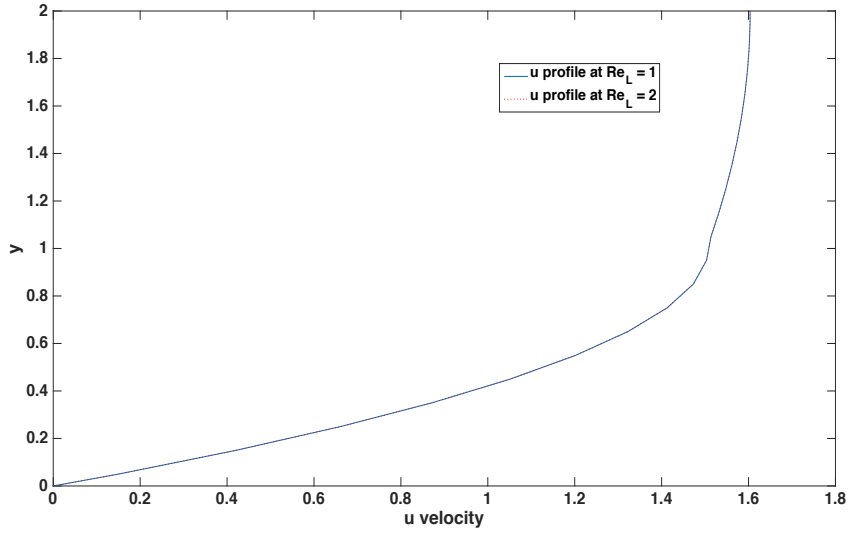

Figure 4.5: horizontal velocity field at different Reynold's number

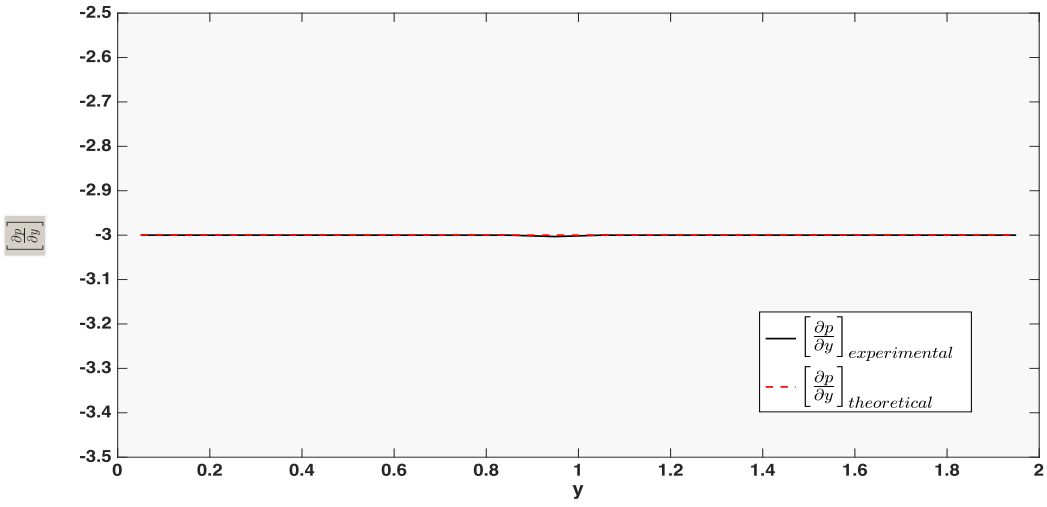

Figure 4.6: Experimental and theoretical pressure gradient, $\left[\frac{\partial p}{\partial y}\right]$, versus y

Chapter 5

Conclusion

In this work, we developed a fluid simulator for steady state solution of a thin film of water flowing down an incline. One of the main objectives of this research was how to capture the evolving interface between air and water, and we used level set method to achieve this. Since, the problem domain was infinite in horizontal direction, we assumed periodicity in this direction with period of 5 and implemented periodic boundary conditions. We described the governing Navier-Stokes equations for fluid motion and discretized them using finite difference method. The discretization had to be done very carefully near the interface because to compute some of the differential terms, the grid points required may lie in different fluids. To achieve this we used interface conditions for both pressure and velocity fields. Once we had the discretized equations, we implemented the fluid solver by following a particular sequence of steps listed in the form of algorithm in Chapter 3. Then we derived some theoretical steady state results for velocity field and pressure, and compared the experimental findings with these theoretical results. We demonstrated that there is a good agreement between the two with few exceptions.

5.1 Future Work

The objective of this research was to analyze steady state of a thin film flow, but in future we would like to analyze non-steady flows which can be achieved by changing the initial conditions to non-zero horizontal and vertical velocity field. By doing so, we would be interested in the evolution of interface with time and expect it to exhibit 'wavy' nature. Also, in the nature and technological applications of thin film flows, the surface over which thin film is flowing is not always smooth (which was the assumption in this work). Instead

the surface can be corrugated, so we will be interested in simulation steady as well as non-steady state flow over such a surface.

References

[1] Christophe Ancey. Plasticity and geophysical flows: A review. *Journal of Non-Newtonian Fluid Mech. 142 (2007) 435*, 2007.

[2] Christophe Ancey. The dynamics of lava flows. *Annual Review of Fluid Mechanics Vol. 32: 477-518*, 2009.

[3] B. Nicholas C. HIrt and N. Romero. A numerical solution algorithm for transient fluid flows. *Technical report*, 1975.

[4] L. Tran Hnel D. O. Gloth and R. Vilsmeier. A front tracking method on unstructured grids. *Computers and Fluids, 32(4):547-570*, 2003.

[5] Joel Ferziger Douglas Enright, Ronald Fedkiw and Ian Mitchell. Level set methods for fluid interfaces. *Journal Computational Physics, 183:83-116*, 2002.

[6] Shaurya Prakash et. al. Nanofluidics: Systems and applications. *IEEE Sensors Journal, VOL. 8, NO. 5*, 2005.

[7] Shaurya Prakash et. al. Nanofluidics: what is it and what can we expect from it? *Microfluid Nanofluid (2005) 1: 249267*, 2005.

[8] R.W. Griffiths. Plasticity and geophysical flows: A review. *Annual Review of Fluid Mechanics Vol. 32: 477-518*, 2000.

[9] A.D. Stroock H.A. Stone and A. Ajdari. Engineering flows in small devices: Microfluidics toward a lab-on-a-chip. *Annu. Rev. Fluid Mech. 2004. 36:381411*, 2004.

[10] C. W. Hirt and B. D. Nichols. Volume of fluid (vof) method for the dynamics of free boundaries. *Journal of Computational Physics, 39(1):201-225*, 1981.

[11] Herbert E Huppert. The propagation of two-dimensional and axisymmetric viscous gravity currents over a rigid horizontal surface. *Journal of Fluid Mechanics*, 121:43–58, 1982.

[12] Herberte Huppert. Gravity currents: a personal perspective. *Journal of Fluid Mechanics (2006), vol. 554, pp. 299322.*, 2006.

[13] Thomas Dornseifer Michael Griebel and Tilman Neunhoeffer. *Numerical Simulation in Fluid Dynamics: A Practical Introduction*. SIAM, 1998.

[14] Christian Beilken Michael Spenke and Thomas Berlage. FOCUS: the interactive table for product comparison and selection. In *Proceedings of the ACM SIGGRAPH/Eurographics Symposium on Computer Animation*, pages 237–245, New York, NY, USA, 2009.

[15] A. A. Nepomnyashchii. Stability of wavy conditions in a film flowing down an inclined plane. *Fluid Dynamics Volume 9, Issue 3, pp 354-359*, 1974.

[16] Alexander A Nepomnyashchy, Manuel G Velarde, and Pierre Colinet. *Interfacial phenomena and convection*. CRC Press, 2001.

[17] S. Osher and J.A. Sethian. Fronts propagating with curvature dependent speed: Algorithms based on hamilton-jacobi formulations. *Journal of Computational Physics, 79, pp.12-49*, 1988.

[18] S. J. Osher and R. P. Fedkiw. *Level Set Methods and Dynamic Implicit surfaces*. Springer, 2003.

[19] Ira M. Cohen Pijush K. Kundu and David R. Dowling. *Fluid Mechanics*. Academic Press, fifth edition, 2011.

[20] Osborne Reynolds. On the theory of lubrication and its application to mr. beauchamp tower's experiments, including an experimental determination of the viscosity of olive oil. *Philosophical Transactions of the Royal Society of London 1 January 1886 vol. 177 157-234*, 1886.

[21] J. P. Pascal S. J. D. D'Alessio and H. A. Jasmine. Instability in gravity-driven flow over uneven surfaces. *Physics of Fluids 21, 062105*, 2009.

[22] J. A. Sethian and P. Smereka. Level set methods for fluid interfaces. *Annual Review Fluid Mechanics 35:341-372*, 2003.

[23] J.A. Sethian. Evolution, implementation and application of level set and fast marching methods for advancing fronts. *Journal of Computational Physics, Volume 169, Issue 2, Pages 503-555*, 2001.

[24] Ronald Fedkiw Stanley Osher. *Level Set Methods and Dynamic Implicit Surfaces*. Springer-Verlag New York, 1 edition, 2008.

[25] Hiroshi Terashima and Gretar Tryggvason. A front-tracking/ghost-fluid method for fluid interfaces in compressible flows. *Journal of Computational Physics, 228(11):4012-4037*, 2009.

[26] Murilo F. Tome and Sean McKee. Gensmac: A computational marker and cell method for free surface flows in general domains. *Journal of Computational Physics Volume 110, Issue 1, January 1994, Pages 171-186*, 1994.

[27] Eleuterio F. Toro. *Riemann Solvers and Numerical Methods for Fluid Dynamics: A Practical Introduction*. Springer, 2009.

[28] S. O. Unverdi and G. Tryggvason. A front tracking method for viscous incompressible multi-fluid flows. *Journal of Computational Physics, 100(1):25-37*, 1992.

[29] B. Merriman Y.C. Chang, T.Y. Hou and S. Osher. A level set formulation of eulerian interface capturing methods for incompressible fluid flows. *Journal Computational Physics, Volume 124, Issue 2*, 1996.